Configurational Properties of Partially Ionized Polyelectrolytes from Monte Carlo Simulation

Herbert H. Hooper,† Harvey W. Blanch, and John M. Prausnitz*

Chemical Engineering Department, University of California, and Materials and Chemical Sciences Division, Lawrence Berkeley Laboratory, 1 Cyclotron Road, Berkeley, California 94720

Received December 11, 1989; Revised Manuscript Received April 10, 1990

ABSTRACT: Monte Carlo simulations have been performed for a lattice model of an isolated, partially ionized polyelectrolyte whose charged groups interact through screened Coulombic potentials. Configurational properties are reported as a function of chain ionization and Debye screening length for chains containing 20–140 segments. At high screening between fixed charges, the chains exhibit power law scaling behavior for the dependence of the mean-square end-to-end distance, $\langle r^2 \rangle$, on chain length. At lower screenings the chains undergo a transformation from flexible to stiff conformations as ionization rises. Long-chain scaling behavior was not observed at low screenings due to the limits on the chain lengths studied here. Simulation results for polyion electrostatic energies and expansion factors are compared with predictions based on the theory of Katchalsky and Lifson and the uniform-expansion extension of this theory. Large discrepancies between theory and simulation are probably due to the assumed theoretical expressions used for describing distance probability distributions between charged groups.

I. Introduction

Solution properties of polymers depend strongly on the conformational behavior of the individual polymer chains. Considerable theoretical, numerical, and experimental effort has been devoted to the study of uncharged polymers, and much is known about their configurational behavior as reviewed in refs 1–3. Polyelectrolytes exhibit a much wider variety of solution properties than uncharged polymers;[4,5] while much theoretical effort has been devoted to the study of charged polymers,[6-19] quantitative understanding of their conformational behavior has not been obtained. The description of polyelectrolyte properties in solution is difficult because of electrostatic interactions in these systems. It is, however, these electrostatic interactions which give polyelectrolytes their rich variety of solution properties that are of significant importance in natural (biological) systems and in numerous technological applications.

Polymer conformational properties are typically described in terms of system length scales. Linear, uncharged polymers are characterized primarily by two length scales: the Kuhn segment length, l, and the chain contour length, L. The mean-square end-to-end distance, $\langle r^2 \rangle$, for uncharged polymers scales as $(L/l)^\eta$ where $\eta = {}^6/_5$ in a good solvent.[1] For polyelectrolytes in solution, additional length scales are important. These length scales include the average distance between charged groups along the chain, $b = L/\nu$ (where ν is the number of charged groups on the polymer), the Debye screening length, κ^{-1}, and the Bjerrum length, $\lambda_B = q^2/DkT$, where q is the charge per group, D is the solution dielectric constant, k is Boltzmann's constant, and T is temperature.

Unlike uncharged polymers, configurational properties of polyelectrolytes are not described by simple scaling laws over a wide range of solution conditions.[14] Instead, polyelectrolytes may assume any shape between that of a random coil or a rigid rod, depending on the system's length scales. Traditional excluded-volume or renormalization-group methods for describing polyelectrolyte configurational properties are often applicable only for limiting cases (i.e., in the unscreened, long-chain limit[10]). However, a number of theories have been suggested for describing the full range of behavior observed in polyelectrolytes. These theories include that of Katchalsky and Lifson,[7,9] self-consistent-field theories,[11] the wormlike chain model,[12,15] renormalization-group techniques,[16,17] and semivariational methods.[18,19] A difficulty in evaluating the accuracy of such analytical theories is that experimental systems are never characterized to the level of detail on which the theories are developed. For example, the number and distribution of ionized groups on a polyelectrolyte (fixed or assumed in analytical theories) is typically not known precisely from experiment.

Computer simulation provides a powerful method for examining configurational properties of model polymer systems under conditions where the system length scales are known exactly because they are specified in the computation. While uncharged polymers have been studied extensively by simulation,[20] relatively few simulation studies have examined polyelectrolyte configurational properties.[21-26] Previous studies have often been concerned with limiting cases in which one or more system length scales are held constant (e.g., completely ionized chains;[23,24] unscreened Coulombic potentials between ionized segments[23]) or where the polyion chains are relatively short.[21,26]

In this work we use Monte Carlo (MC) simulation to study configurational properties of isolated polyelectrolytes as a function of polyion chain length, charge density, and screening between fixed ions. We investigate an idealized, lattice representation of a polyion, which neglects high-resolution details of polyelectrolyte behavior (i.e., counterion interactions, effects of side groups on structure). However, the simplicity of the model allows us to study a larger region of phase space (range of system length scales) than would be possible in a more detailed study. Simulation results are compared with predictions of the Katchalsky–Lifson polyelectrolyte-expansion theory[7] and with the extended uniform-expansion version of this model.[9,11]

* To whom correspondence should be addressed.
† Present address: Air Products and Chemicals, Allentown, PA 18195.

0024-9297/90/2223-4820$02.50/0

II. Simulation Method

A. Model Description. The polyelectrolyte is modeled as a self-avoiding walk (SAW) of $N-1$ steps (N segments) on a cubic lattice. The distance between lattice sites, l, is 2.52 Å, which is the distance between alternate atoms on a carbon-backbone chain assuming tetrahedral geometry and a carbon–carbon bond length of 1.54 Å.[24] In this work, the only energetic interactions are Coulombic forces between ionized monomers. Short-range attractive interactions between neighboring (nonbonded) monomers are not considered, which is equivalent to assuming that the interchange energy between the polymer segments and the surrounding medium is zero. In a forthcoming paper[27] we explore the effect of polymer hydrophobicity (i.e., attractive monomer–monomer interactions) on polyelectrolyte conformational properties.

The fractional ionization of the polymer chain, λ, is varied from 0 (no charged monomers) to 1.0 (all monomers ionized). For a given λ, the location of charged segments is determined by considering the chain to continue infinitely in both directions (or, equivalently, considering the two chain ends to be joined in a closed loop) and spacing the charges uniformly along the infinite chain (or loop). For example, consider a 10-segment chain with $\lambda = 0.20$ (two ionized segments). The number of uncharged segments between ionized segments must then be 4. To fix the *positions* of these ionized segments, we impose symmetry of charged-bead locations with respect to the chain center. Thus, for our example, the first charged segment is placed at position 3, and the second charged segment, at position 8. The value of λ is not varied continuously but in correspondence with *discrete* and *uniform* separations between ionized segments. We start with $\lambda = 1.0$ (all segments ionized) and then insert one uncharged segment between ionized segments ($\lambda = 0.50$), two uncharged segments ($\lambda = 0.67$), etc.

Counterions are not considered explicitly here, nor do we consider the detailed nature of the ionic atmosphere surrounding the polyion. Instead, every charged monomer on the chain interacts with every other charged monomer through a screened Debye–Hückel Coulombic potential[28]

$$u_{ij} = \frac{z_i z_j e^2}{D r_{ij}} \exp(-\kappa r_{ij}) \tag{1}$$

where u_{ij} is the potential between monomers i and j, which have charges $z_i e$ and $z_j e$ and are separated by a distance r_{ij}. The dielectric constant, D, is taken as that of water at 25 °C. The inverse Debye screening length, κ, is given by[28]

$$\kappa^2 = \frac{4\pi e^2 N_A \sum_i z_i^2 C_i}{DkT} \tag{2}$$

where N_A is Avagadro's number and C_i is the concentration of ionic species i. Because we consider the polyelectrolyte at infinite dilution, the sum in eq 2 is over the species of *added* electrolyte and does not include the charges on the polymer or the counterions.[24] Our course-grained model considers specifically only ions that are on the polymer backbone. The presence of added electrolyte influences polyion properties through the screening length, which depends on ionic strength.

Our polyelectrolyte model is simple and neglects some subtle, but often important, features of a real polyelectrolyte in solution. Most significant is our choice to "smear out" the details of the unbound ions in solution. Certain characteristics of polyelectrolyte behavior, such as counterion condensation,[8] will thus not be observed here. In addition, the "true" potential between fixed ions, as determined by the radial distribution of mobile ions around each polymer charge, is replaced here by a screened Coulombic potential. It will be useful to examine more detailed polyelectrolyte models that consider counterions and added electrolyte explicitly in the simulation. However, as shown by Valleau,[26] the added complexities (and computation requirements) of such a detailed model limit the range of length scales (particularly the length of the polyion) that can be examined.

While not an exact representation of a polyelectrolyte in solution, we have chosen here a model that contains the essential physics of polyion expansion. Most analytical theories of polyelectrolyte expansion also assume screened Coulombic potentials between charged ions; even this simple representation of a polyion is not completely understood. The results of this work can thus be used for testing predictions (and assumptions) of these analytical theories.

B. Sampling Procedure. Ensemble-average chain properties were determined by Metropolis Monte Carlo sampling[29] over the configurational space of the polyelectrolyte. Successive chain configurations were generated by using the "reptation" method.[30] In this procedure, one end of the chain is randomly designated as the head and is allowed to advance (in a randomly chosen direction) one lattice position. In practice, this movement is usually effected by "removing" the last segment (from the chain tail) and adding it to the chain head in a random direction. This breaking and adding of end segments is simply a mechanism for allowing the chain to "slither" through configurational space and does not imply actual breaking of chain bonds. For polymers in which all segments are identical (i.e., uncharged or fully ionized chains), the movement of internal segments is implicit; i.e., adding the chain tail to the head gives the impression that all chain segments have advanced one lattice position. However, for chains in which all segments are *not* identical (i.e., partially ionized polyelectrolytes), adding the chain tail to the head would result in a change of position of the ionized beads along the chain backbone. In this work, we advance *each* segment during reptation moves to retain the chemical identity of the chain during sampling.

The energy of chain configuration s, E_s, is given by the sum of the potentials u_{ij} between all segment pairs

$$E_s = \sum_{i}^{N-1} \sum_{j=i+1}^{N} u_{ij} \tag{3}$$

where N is the number of chain segments. The potential between ionized segments is given by eq 1; if either i or j (or both) is uncharged, $u_{ij} = 0$. Trial chain conformations (generated by reptation) are accepted based on the probability

$$p_{s+1} = \min\{1, \exp(-\Delta E/kT)\} \tag{4}$$

where ΔE is the energy change in going from configuration s to configuration $s+1$ (i.e., $\Delta E = E_{s+1} - E_s$). For an attempted move from state s to state $s+1$, if the chain energy is lowered or remains unchanged ($\Delta E \leq 0$), the move is always accepted. However, if $\Delta E > 0$, the move is accepted with probability $\exp(-\Delta E/kT)$. When a trial move is rejected, the previous conformation is kept and considered as a 'new' state in the ensemble averages.

Starting with an initial chain configuration, approximately N^2 reptation cycles are required to generate a new configuration which is uncorrelated with the original one.[24] Thus, the simulation is divided into *blocks* of order

Table I
Number of Monte Carlo Cycles and Division of Cycles into Blocks

no. of chain beads, N	no. of cycles per block	no. of blocks	total no. of Monte Carlo cycles
20	1000	200	200 000
40	4000	200	800 000
60	5000	150	750 000
100	10000	100	1 000 000
140	20000	100	2 000 000

N^2 configurations. The chain is relaxed from its initial state by allowing the system to evolve through five blocks of configurations. The exact nature of the initial state is unimportant, because this configuration is forgotten during the relaxation process (which is not considered when determining ensemble averages). Following chain relaxation, average chain properties are recorded for each additional block; at the end of the simulation, these block averages are used for estimating ensemble-average properties. For the five chain lengths studied here, Table I shows the organization of the simulation (i.e., number of cycles per block and number of blocks) along with the total number of configurations generated.

C. Conformational Properties and Distribution Functions. Using the MC sampling technique described in the previous section, we calculate several polyion conformational characteristics. The size of the polyelectrolyte chain is characterized by the mean-square end-to-end distance

$$\langle r^2 \rangle = \langle (\mathbf{r}_n - \mathbf{r}_1)^2 \rangle \tag{5}$$

and by the mean-square radius of gyration

$$\langle s^2 \rangle = \frac{1}{N} \langle \sum_{i=1}^{N} (\mathbf{r}_i - \mathbf{r}_{cm})^2 \rangle \tag{6}$$

where $\mathbf{r}_i$ is the position vector locating the ith bead (segment) of the chain, and $\mathbf{r}_{cm}$ is the vector locating the center of mass of the chain. Here, $\langle\ \rangle$ denotes an ensemble average over a Monte Carlo run. We also calculate the ensemble-average energy of the chain, $\langle E \rangle$, which is simply the average of eq 3 taken over all blocks in a run. Standard errors of ensemble-average properties are estimated by using the method of Smith and Wells.[31]

A quantity often discussed for polymers with inherent stiffness is the persistence length, L_p. This characteristic length represents the distance over which directional correlation of the chain persists and is equal to $^1/_2$ the Kuhn segment length.[1] L_p can be calculated from the distribution of angles of polyion bonds relative to the central bond,[24] i.e.

$$L_p = l \sum_{k=1}^{N/2-1} \langle \cos \phi_k \rangle \tag{7}$$

where ϕ_k is the angle between the central (cth) bond and the ($c + k$)th bond, and the index k varies from 0 (at the central bond) to $N/2 - 1$ at the chain end.

In addition to *mean* values of polymer configurational properties, the *distribution* functions for these averages also play an important role in determining some polymer characteristics. We calculate here the probability distribution function for the end-to-end distance by doing a frequency count for discretized distance intervals (for each block) and normalizing the area under the distribution curve. These distributions are discussed in the last section.

Table II
Simulation Results for Uncharged Self-Avoiding Walks[a]

N	$\langle r^2 \rangle/(N-1)^2 l^2$	$\langle s^2 \rangle/(N-1) l^2$	L_p
20	0.100 (0.001)	0.306 (0.003)	1.42 (0.05)
40	0.0563 (0.0006)	0.349 (0.004)	1.83 (0.05)
60	0.0411 (0.0008)	0.384 (0.005)	2.16 (0.09)
100	0.0260 (0.0007)	0.416 (0.009)	2.38 (0.16)
140	0.0203 (0.0005)	0.442 (0.009)	2.59 (0.14)

[a] N = no. of chain beads. l = lattice bond length (2.52 Å). $\langle r^2 \rangle$, $\langle s^2 \rangle$, and L_p defined in eqs 5–7. Results in parentheses represent standard errors.

III. Simulation Results

Two limiting cases of the model were analyzed to verify the accuracy of the program. First, we considered uncharged (athermal) SAW's on the cubic lattice. Table II presents our results for $\langle r^2 \rangle$, $\langle s^2 \rangle$, and L_p in this limit for chains of length 20–140 segments. The results for $\langle r^2 \rangle$ follow the scaling relation $\langle r^2 \rangle \approx N^{1.2}$, in agreement with the known properties of this well-studied case.[1] For *fully* ionized chains in the *unscreened* limit, we compared our results with the lattice simulation studies of Baumgartner;[23] good agreement is also obtained in this limit.

Configurational properties were calculated for isolated, partially ionized polyelectrolytes of length 20, 40, 60, 100, and 140 segments. The degree of chain ionization, λ, was varied from 0 to 1.0 for all cases except the 140-segment chains; due to large computation requirements, we studied this chain only up to $\lambda = 0.33$. Tables III–VI present results for the mean electrostatic energy, $\langle E \rangle/kT$, reduced values of $\langle r^2 \rangle$ and $\langle s^2 \rangle$, and the persistence length, L_p. The Debye screening length was set to values corresponding to added 1:1 electrolyte concentrations of 1.0 M (κ^{-1} = 3.04 Å), 0.1 M (κ^{-1} = 9.62 Å), 0.01 M (κ^{-1} = 30.4 Å), 0.001 M (κ^{-1} = 96.2 Å), and the unscreened limit ($\kappa^{-1} = \infty$).

Figures 1–4 present the chain length dependence of the reduced mean-square end-to-end distances at screening lengths corresponding to ionic strengths between 1.0 and 0.001 M. Results for $\kappa^{-1} = \infty$ are not presented graphically because, for the chain lengths studied here, results in 0.001 M electrolyte (Figure 4) are nearly identical with those in the unscreened limit. Figures 1–4 illustrate the rich variety of configurational behaviors observed for polyelectrolytes as a function of system length scales. The magnitude of $\langle r^2 \rangle/(N-1)^2 l^2$ is bounded, at the upper limit, by the rigid-rod value of 1.0 and, at the lower limit, by the uncharged, SAW result (given in Table II and shown graphically in Figures 1–4). The scaling behavior for polyelectrolytes (in the long-chain limit) also has well-defined bounds. Fully ionized, unscreened polyelectrolytes are known to exhibit rigid-rod scaling behavior[23] ($\langle r^2 \rangle \approx N^2$), which would appear as a horizontal line on Figures 1–4. SAW's follow the $\langle r^2 \rangle \approx N^{1.2}$ relation, which, in Figures 1–4, would be represented by a decaying line of approximate slope −0.82 (as for chains with 0% charge). Here we consider our results for partially ionized chains in light of these well-understood limiting cases.

At an equivalent 1:1 electrolyte concentration of 1.0 M (Figure 1), the screening length (3.04 Å) is similar in magnitude to the segment bond lengths, and repulsions between fixed charges are highly screened. Thus, for lightly ionized polyelectrolytes (e.g., 10% charge) the spacing between charges on the chain is much greater than κ^{-1}, and the configurational statistics are perturbed little from the uncharged (SAW) case. Ionizations greater than 10% result in chain expansion with respect to the uncharged case; however, all of the ionized chains exhibit decaying scaling behavior in this high-screening limit. For any finite

Table III
Electrostatic Energy ($\langle E \rangle / kT$) of Partially Ionized Polyelectrolyte Chains

			ionic strength, M (concn of added 1:1 electrolyte)				
N^a	NIB[b]	λ^c	1.0	0.1	0.01	0.001	0[d]
20	2	0.10	0.052 (0.001)	0.265 (0.003)	0.498 (0.004)	0.629 (0.004)	0.703 (0.004)
	5	0.25	1.04 (0.01)	3.66 (0.02)	6.14 (0.03)	7.38 (0.03)	8.03 (0.03)
	10	0.50	6.71 (0.03)	18.1 (0.1)	28.5 (0.1)	33.8 (0.11)	36.5 (0.1)
	20	1.0	38.2 (0.1)	81.4 (0.2)	117.1 (0.2)	137.6 (0.1)	151.1 (0.2)
40	4	0.10	0.176 (0.003)	0.968 (0.009)	2.00 (0.01)	2.69 (0.02)	3.09 (0.02)
	10	0.25	2.46 (0.02)	9.11 (0.05)	15.9 (0.1)	20.0 (0.11)	22.8 (0.1)
	20	0.50	14.3 (0.1)	39.8 (0.1)	65.3 (0.2)	82.6 (0.3)	93.2 (0.3)
	40	1.0	78.7 (0.2)	171.4 (0.3)	251.9 (0.3)	310.8 (0.6)	360.9 (0.6)
60	6	0.10	0.314 (0.006)	1.74 (0.02)	4.02 (0.04)	5.59 (0.04)	6.59 (0.04)
	15	0.25	3.89 (0.04)	14.2 (0.1)	26.3 (0.1)	35.0 (0.2)	42.1 (0.2)
	30	0.50	21.5 (0.1)	62.4 (0.3)	103.7 (0.4)	131.2 (0.6)	154.3 (0.6)
	60	1.0	121.2 (0.2)	251.6 (0.7)	381.0 (1.0)	511.8 (0.7)	610.3 (0.9)
100	5	0.05	0.068 (0.003)	0.643 (0.012)	1.61 (0.02)	2.56 (0.03)	3.14 (0.03)
	10	0.10	0.574 (0.012)	3.47 (0.06)	8.40 (0.10)	12.0 (0.1)	14.3 (0.1)
	20	0.20	3.88 (0.07)	16.2 (0.2)	30.4 (0.3)	43.4 (0.2)	54.3 (0.2)
	25	0.25	7.14 (0.09)	25.3 (0.2)	47.2 (0.3)	67.0 (0.3)	84.4 (0.4)
	50	0.50	36.8 (0.2)	106.0 (0.39)	179.0 (0.6)	233.5 (1.2)	309.9 (1.1)
	100	1.0	204.0 (0.4)	409.0 (1.8)	661.3 (1.7)	906.7 (1.6)	1162.1 (1.6)
140	7	0.05	0.100 (0.003)	0.889 (0.018)	2.61 (0.05)	4.37 (0.05)	5.63 (0.06)
	14	0.10	0.802 (0.015)	5.06 (0.07)	12.2 (0.1)	15.7 (0.2)	19.1 (0.3)
	28	0.20	5.56 (0.08)	21.1 (0.3)	43.9 (0.3)	65.8 (0.4)	83.5 (0.3)
	47	0.33	18.1 (0.2)	61.4 (0.6)	118.3 (0.4)	173.4 (0.3)	217.7 (0.7)

[a] Number of chain beads. [b] Number of ionized beads. [c] Fraction of chain beads that are ionized. [d] Unscreened Coulombic potential between ionized beads. Results in parentheses represent standard errors.

Table IV
Reduced Mean-Square End-to-End Distance ($\langle r^2 \rangle / (N-1)^2 l^2$) of Partially Ionized Polyelectrolyte Chains

			ionic strength, M (concn of added 1:1 electrolyte)				
N^a	NIB[b]	λ^c	1.0	0.1	0.01	0.001	0[d]
20	2	0.10	0.101 (0.001)	0.105 (0.001)	0.108 (0.001)	0.108 (0.001)	0.106 (0.001)
	5	0.25	0.116 (0.001)	0.143 (0.002)	0.156 (0.002)	0.160 (0.002)	0.158 (0.002)
	10	0.50	0.163 (0.002)	0.225 (0.003)	0.286 (0.004)	0.293 (0.003)	0.310 (0.004)
	20	1.0	0.255 (0.003)	0.608 (0.007)	0.799 (0.004)	0.836 (0.003)	0.826 (0.004)
40	4	0.10	0.0597 (0.0007)	0.0670 (0.0008)	0.0731 (0.0009)	0.0723 (0.0009)	0.0727 (0.0010)
	10	0.25	0.0721 (0.0009)	0.111 (0.002)	0.146 (0.002)	0.149 (0.002)	0.155 (0.002)
	20	0.50	0.103 (0.002)	0.222 (0.003)	0.317 (0.004)	0.374 (0.005)	0.404 (0.005)
	40	1.0	0.176 (0.002)	0.584 (0.009)	0.898 (0.002)	0.919 (0.001)	0.922 (0.001)
60	6	0.10	0.0432 (0.0009)	0.0523 (0.0009)	0.0599 (0.0013)	0.0611 (0.0013)	0.0612 (0.0013)
	15	0.25	0.0554 (0.0011)	0.100 (0.002)	0.145 (0.002)	0.166 (0.003)	0.162 (0.003)
	30	0.50	0.0821 (0.0021)	0.192 (0.004)	0.354 (0.006)	0.456 (0.007)	0.473 (0.009)
	60	1.0	0.134 (0.003)	0.608 (0.013)	0.932 (0.001)	0.945 (0.001)	0.950 (0.001)
100	5	0.05	0.0267 (0.0007)	0.0291 (0.0008)	0.0336 (0.0008)	0.0328 (0.0008)	0.0358 (0.0009)
	10	0.10	0.0283 (0.0009)	0.0380 (0.0011)	0.0498 (0.0014)	0.0576 (0.0016)	0.0606 (0.0018)
	20	0.20	0.0360 (0.0012)	0.0667 (0.0022)	0.108 (0.003)	0.131 (0.003)	0.142 (0.003)
	25	0.25	0.0381 (0.0013)	0.0800 (0.0025)	0.143 (0.003)	0.176 (0.004)	0.190 (0.003)
	50	0.50	0.0578 (0.0022)	0.164 (0.004)	0.377 (0.007)	0.544 (0.007)	0.517 (0.006)
	100	1.0	0.0866 (0.0030)	0.610 (0.016)	0.955 (0.001)	0.968 (0.001)	0.970 (0.004)
140	7	0.05	0.0207 (0.0005)	0.0236 (0.0007)	0.0287 (0.0009)	0.0285 (0.007)	0.0304 (0.0009)
	14	0.10	0.0218 (0.0006)	0.0306 (0.0009)	0.0478 (0.0013)	0.0585 (0.001)	0.0628 (0.0017)
	28	0.20	0.0269 (0.0012)	0.0518 (0.0023)	0.109 (0.003)	0.131 (0.003)	0.161 (0.003)
	47	0.33	0.0331 (0.0017)	0.113 (0.004)	0.187 (0.004)	0.252 (0.005)	0.349 (0.004)

[a-d] See footnotes in Table III.

screening length, flexible-chain scaling behavior ($\langle r^2 \rangle \approx N^{1.2}$) must be approached in the long-chain limit, i.e., as the contour length becomes much larger than κ^{-1}. Due to the low value of κ^{-1} in Figure 1, we are near the long-chain limit for all degrees of ionization.

At κ^{-1} = 9.62 Å (Figure 2), the polyions expand significantly more with increasing ionization than those shown in Figure 1. Also, we do not observe in Figure 2 decaying scaling behavior for chains at high degrees of ionization; instead, the polyions undergo a transformation from flexible-chain behavior at low ionization to rigid-rod behavior at full ionization. This transformation is due to the comparable magnitudes of κ^{-1} and charge-separation distances and indicates that, for the highly ionized chains, we are observing only "intermediate" length-dependent behavior (i.e., not the long-chain limiting scaling properties). Even fully ionized chains, which are locally rodlike (i.e, stiff for length scales comparable to κ^{-1}), will appear flexible when viewed on length scales much greater than κ^{-1} (as seen in Figure 1).

Figures 3 and 4 illustrate, respectively, the strong charge dependence of polyion expansion observed at κ^{-1} = 30.4 Å and κ^{-1} = 96.2 Å. These results are similar to those seen in Figure 2; however, the length dependence of $\langle r^2 \rangle$ here is more complex than that observed at κ^{-1} = 9.62 Å. For short chains with $\lambda > 0.25$, $\langle r^2 \rangle / (N-1)^2 l^2$ first increases with increasing chain length and then appears to approach an upper limit where rigid-rod scaling behavior is observed. Carnie et al.[24] observed similar behavior for fully ionized polyelectrolytes at short chain lengths. Their explanation is that the addition of charges to a short chain increases the field exerted by the chain ends on the chain center and stiffens this central region, thereby increasing the rodlike character of the chain. This behavior should be observed

Table V
Reduced Mean-Square Radius of Gyration ($\langle s^2 \rangle / (N-1)l^2$) of Partially Ionized Polyelectrolyte Chains

			ionic strength, M (concn of added 1:1 electrolyte)				
N^a	NIB[b]	λ^c	1.0	0.1	0.01	0.001	0[d]
20	2	0.10	0.307 (0.002)	0.318 (0.003)	0.326 (0.003)	0.325 (0.003)	0.320 (0.003)
	5	0.25	0.343 (0.003)	0.398 (0.003)	0.424 (0.004)	0.433 (0.005)	0.432 (0.004)
	10	0.50	0.439 (0.004)	0.605 (0.006)	0.678 (0.008)	0.696 (0.007)	0.732 (0.008)
	20	1.0	0.637 (0.005)	1.29 (0.01)	1.57 (0.006)	1.62 (0.004)	1.61 (0.005)
40	4	0.10	0.367 (0.003)	0.400 (0.004)	0.427 (0.004)	0.425 (0.004)	0.427 (0.005)
	10	0.25	0.426 (0.004)	0.604 (0.007)	0.740 (0.009)	0.753 (0.008)	0.778 (0.009)
	20	0.50	0.583 (0.007)	1.06 (0.01)	1.44 (0.015)	1.64 (0.02)	1.78 (0.02)
	40	1.0	0.914 (0.009)	2.42 (0.03)	3.31 (0.01)	3.34 (0.01)	3.35 (0.01)
60	6	0.10	0.399 (0.006)	0.470 (0.007)	0.518 (0.009)	0.528 (0.009)	0.530 (0.009)
	15	0.25	0.496 (0.007)	0.802 (0.014)	1.07 (0.01)	1.20 (0.02)	1.17 (0.02)
	30	0.50	0.702 (0.012)	1.40 (0.02)	2.32 (0.03)	2.92 (0.04)	3.06 (0.04)
	60	1.0	1.08 (0.003)	3.74 (0.05)	5.00 (0.01)	5.02 (0.01)	5.04 (0.01)
100	5	0.05	0.416 (0.009)	0.443 (0.009)	0.502 (0.010)	0.499 (0.011)	0.530 (0.012)
	10	0.10	0.449 (0.011)	0.568 (0.013)	0.695 (0.014)	0.779 (0.017)	0.807 (0.018)
	20	0.20	0.531 (0.014)	0.910 (0.021)	1.34 (0.02)	1.58 (0.02)	1.59 (0.02)
	25	0.25	0.563 (0.015)	1.10 (0.02)	1.72 (0.03)	2.03 (0.03)	2.07 (0.03)
	50	0.50	0.855 (0.020)	1.99 (0.03)	4.01 (0.05)	5.31 (0.06)	4.99 (0.05)
	100	1.0	1.27 (0.03)	6.10 (0.11)	8.32 (0.01)	8.37 (0.004)	8.38 (0.01)
140	7	0.05	0.462 (0.009)	0.510 (0.010)	0.591 (0.015)	0.600 (0.012)	0.612 (0.013)
	14	0.10	0.479 (0.010)	0.629 (0.014)	0.914 (0.021)	1.07 (0.02)	1.16 (0.03)
	28	0.20	0.576 (0.017)	1.01 (0.03)	1.79 (0.03)	2.13 (0.04)	2.55 (0.03)
	47	0.33	0.716 (0.023)	1.89 (0.05)	3.01 (0.04)	3.81 (0.04)	5.05 (0.04)

[a-d] See footnotes in Table III.

Table VI
Persistence Length, L_p (in Angstroms) of Partially Ionized Polyelectrolyte Chains

			ionic strength, M (concn of added 1:1 electrolyte)				
N^a	NIB[b]	λ^c	1.0	0.1	0.01	0.001	0[d]
20	2	0.10	1.40 (0.04)	1.56 (0.04)	1.69 (0.05)	1.70 (0.05)	1.62 (0.05)
	5	0.25	1.98 (0.05)	2.86 (0.06)	3.20 (0.07)	3.40 (0.08)	3.33 (0.07)
	10	0.50	3.25 (0.07)	5.70 (0.11)	6.78 (0.14)	6.91 (0.13)	7.69 (0.14)
	20	1.0	5.90 (0.09)	15.5 (0.2)	19.7 (0.1)	20.4 (0.1)	20.1 (0.1)
40	4	0.10	2.06 (0.05)	2.50 (0.07)	2.91 (0.07)	2.92 (0.07)	2.97 (0.08)
	10	0.25	2.77 (0.08)	5.30 (0.14)	7.24 (0.16)	7.40 (0.15)	7.95 (0.17)
	20	0.50	4.82 (0.13)	11.8 (0.2)	17.4 (0.3)	20.7 (0.3)	23.0 (0.4)
	40	1.0	8.85 (0.15)	30.9 (0.5)	45.1 (0.1)	45.8 (0.1)	45.8 (0.1)
60	6	0.10	2.33 (0.11)	3.31 (0.12)	4.00 (0.14)	4.18 (0.16)	4.30 (0.14)
	15	0.25	3.72 (0.14)	8.00 (0.29)	11.9 (0.3)	14.1 (0.3)	14.0 (0.3)
	30	0.50	6.59 (0.27)	15.3 (0.4)	26.0 (0.6)	39.2 (0.7)	41.2 (0.7)
	60	1.0	10.3 (0.3)	46.6 (1.0)	70.3 (0.1)	70.9 (0.1)	71.2 (0.1)
100	5	0.05	2.33 (0.14)	2.79 (0.15)	3.49 (0.18)	3.62 (0.17)	4.16 (0.19)
	10	0.10	2.81 (0.18)	4.24 (0.24)	6.08 (0.29)	7.54 (0.29)	7.78 (0.4)
	20	0.20	3.88 (0.27)	7.69 (0.53)	14.8 (0.5)	18.9 (0.4)	20.4 (0.6)
	25	0.25	4.06 (0.29)	11.7 (0.5)	20.6 (0.5)	24.7 (0.8)	25.7 (0.6)
	50	0.50	7.83 (0.55)	24.2 (0.9)	54.6 (1.4)	76.7 (1.1)	66.8 (1.4)
	100	1.0	11.3 (0.47)	83.8 (2.0)	120.3 (0.2)	121.4 (0.1)	121.6 (0.1)
140	7	0.05	2.76 (0.15)	3.56 (0.19)	4.81 (0.26)	5.06 (0.21)	5.08 (0.22)
	14	0.10	3.04 (0.17)	4.78 (0.27)	9.04 (0.39)	11.4 (0.3)	13.1 (0.5)
	28	0.20	4.27 (0.36)	9.25 (0.60)	19.4 (0.9)	26.1 (0.8)	34.8 (0.9)
	47	0.33	5.78 (0.53)	18.9 (1.4)	34.6 (1.8)	54.9 (1.6)	67.0 (1.6)

[a-d] See footnotes in Table III.

only in cases where the screening length is longer than, or comparable to, the contour length. The results in Figures 3 and 4 for chains with $\lambda > 0.25$ appear to follow this explanation. Rigid-rod scaling behavior is observed for these chains when the contour length increases beyond the point where end beads continue to influence the chain centers. The long-chain, flexible-scaling limit (i.e., contour length $\gg \kappa^{-1}$) is not observed for the ionized chains in Figures 3 and 4.

Figure 5 presents the length dependence of the ratio $\langle s^2 \rangle / \langle r^2 \rangle$ at screening length $\kappa^{-1} = 30.4$ Å (considered in Figure 3). This dimensionless ratio characterizes polymer shape and varies (for 3-dimensional chains) from 0.155 for self-avoiding walks[22] to 0.083 for rigid rods (refs 22 and 24 incorrectly state that the limiting, rigid-rod value is 0.100). Thus, Figure 5 provides additional information regarding the effect of chain length on polyion shape at $\kappa^{-1} = 30.4$ Å. Despite the nonmonotonic behavior of the reduced end-to-end distance seen in Figure 3, Figure 5 clearly indicates a tendency for all of the chains at this screening length to assume increasing rodlike structure with increasing chain length. This decrease of $\langle s^2 \rangle / \langle r^2 \rangle$ cannot continue beyond the rigid-rod limit of 0.083; it appears to level off for the longer chains studied.

Figures 1–5 illustrate the effect of chain length and ionization on polyion expansion for different screening lengths. For a chain length of 100 beads, Figure 6 shows the large effect of screening on chain expansion. The ionized chains decrease in size as ionic strength increases; this decrease is particularly dramatic for highly ionized chains, which undergo order-of-magnitude size transitions in the concentration range 0.01–1.0 M.

Figure 7 presents persistence lengths for partially ionized chains at $\kappa^{-1} = 3.04$ and 96.2 Å. Persistence length

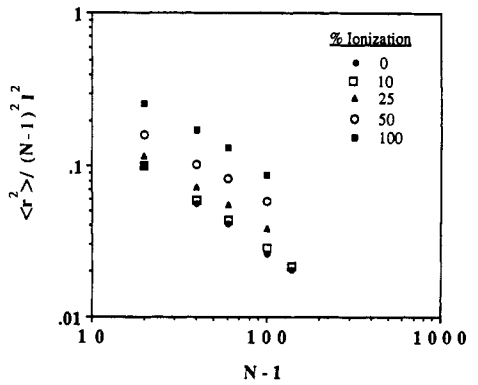

Figure 1. Chain length dependence of reduced mean-square end-to-end distance for different degrees of ionization at screening length κ^{-1} = 3.04 Å. The upper bound of the ordinate ($\langle r^2 \rangle / (N-1)^2 l^2 = 1.0$) corresponds to a fully extended (rodlike) configuration.

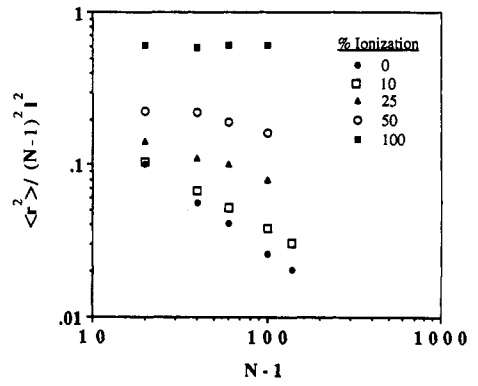

Figure 2. Chain length dependence of polyelectrolyte expansion at screening length κ^{-1} = 9.62 Å.

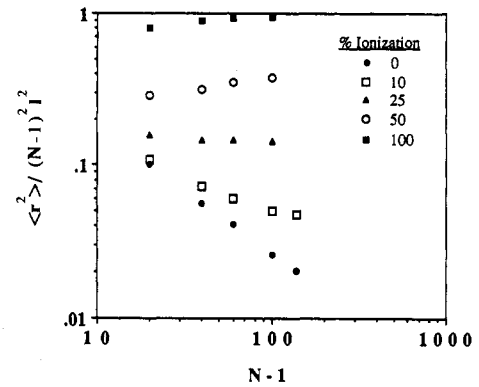

Figure 3. Chain length dependence of polyelectrolyte expansion at screening length κ^{-1} = 30.4 Å.

characterizes chain stiffness; it is calculated from the directional correlations of neighboring bonds about the central bond. At κ^{-1} = 3.04 Å (Figure 7a), the chains are not highly extended, and persistence lengths are similar in magnitude to those of uncharged chains. However, at low screening (Figure 7b), the chains expand significantly with increasing ionization, and large persistence lengths are observed. In addition, the chain length dependence of the persistence length is much larger at κ^{-1} = 96.2 Å than at κ^{-1} = 3.04 Å. This larger dependence is due to the relative magnitudes of κ^{-1} and the contour length, which results in the chains at κ^{-1} = 3.04 Å behaving much closer to the long-chain limit than chains at κ^{-1} = 96.2 Å. Carnie et al.[24] discuss a procedure for estimating infinite-chain persistence lengths from an extrapolation of the cosine-distribution data for chains of finite length.

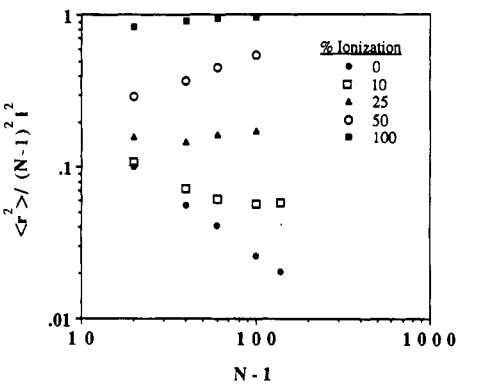

Figure 4. Chain length dependence of polyelectrolyte expansion at screening length κ^{-1} = 96.2 Å.

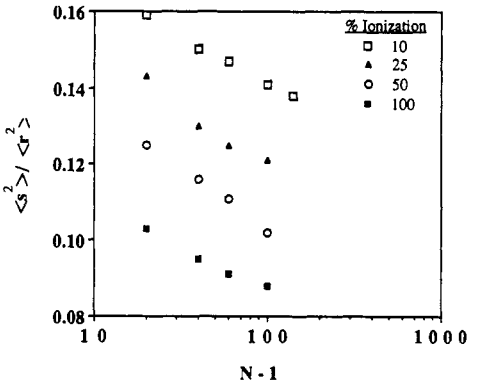

Figure 5. Chain length dependence of shape parameter $\langle s^2 \rangle / \langle r^2 \rangle$ at κ^{-1} = 30.4 Å. The monotonic decrease in $\langle s^2 \rangle / \langle r^2 \rangle$ (for all chains) indicates increasing rodlike character with increasing chain length. For fully extended chains, $\langle s^2 \rangle / \langle r^2 \rangle$ = 0.083.

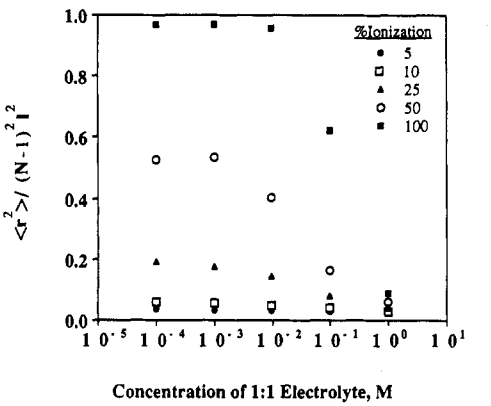

Figure 6. Dependence of mean-square end-to-end distance (for 100-segment chains) on screening length, expressed here as a concentration of 1:1 electrolyte.

IV. Comparison with Theory

The results shown in the previous section indicate that polyelectrolyte configurational properties depend on system length scales in a nontrivial manner. While a number of theories (section I) have been proposed for describing this dependence, we are not aware of any comparisons of theory with simulation results for model systems. We cannot, in a single paper, provide a detailed comparison of our simulation results with all relavent analytical theories. Instead, we compare our results with one theory, both for its own interest and as an example of the information that can be obtained from such a comparison.

We consider here the theory of Katchalsky and Lifson[7] and the *uniform-expansion* extension of this theory.[9,11] Katchalsky–Lifson (K-L) theory, while admittedly old, offers an instructive comparison with our simulation results

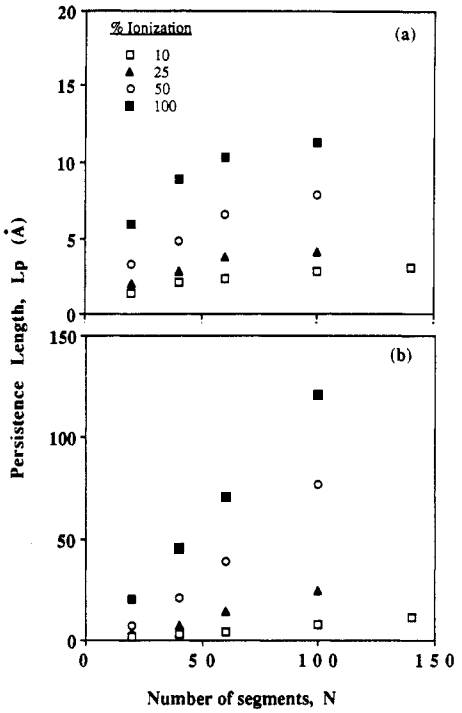

Figure 7. Chain length dependence of persistence length for partially ionized polyelectrolytes: (a) screening length κ^{-1} = 3.04 Å; (b) screening length κ^{-1} = 96.2 Å.

for two reasons. First, the K–L polyelectrolyte model is directly analogous to the model used in our simulation: a flexible chain with fixed charges distributed evenly along the backbone interacting with each other via screened Coulombic potentials. Thus, any discrepancies between simulation and theory must result from assumptions made in the theory, as opposed to differences in the physical models of the two approaches.

Second, our motivation for considering K–L theory is that this theory is still used fairly often (and with little justification) for describing the electrostatic contribution to the free energy of polyelectrolyte solutions[7] and cross-linked polyelectrolyte gels.[32] The latter case is of particular interest to us, as we have been investigating experimentally and theoretically the swelling properties of cross-linked polyelectrolyte hydrogels.[33,34] Several authors[32] have developed gel-swelling models which use the K–L expression for describing the contribution of intrachain fixed-ion repulsions to the Gibbs energy change of swelling. Because this contribution can be large, and can potentially mask other contributions (such as polymer–solvent mixing effects), we believe it is important to inquire whether the predictions of K–L theory truly represent the physical model upon which that theory is based.

To facilitate our comparison, we provide here a brief overview of the K–L derivation. The polyion electrostatic energy, F_{el}, is given as a sum over potentials between all ion pairs

$$F_{el} = \nu^2 \int_0^1 (1-\xi)\, \bar{u}(\xi)\, d\xi \tag{8}$$

where ν is the number of fixed charges on the chain, ξ is the fraction of the contour length that separates fixed charges i and j, i.e., $\xi = |i-j|/\nu$, and $\bar{u}(\xi)$ represents the *mean* potential between fixed charges as a function of ξ. For a given separation distance, r, between ends of the polymer chain, the distance between charged segments i and j is *not* fixed but follows a probability distribution. Here, $W(h;\xi,r)$ represents the probability of finding a distance h between two charged segments i and j when the polyion end-to-end distance is r. Thus, the *mean* potential between charges i and j is

$$\bar{u}_{ij} = \int_0^\infty W(h;\xi,r)\, u_{ij}\, dh \tag{9}$$

where the potential u_{ij} is given by eq 1.

Thus far, the K–L derivation corresponds exactly to our simulation model, and F_{el} is comparable with $\langle E_{el}\rangle$ computed in the simulation. To proceed, however, it is necessary to assume a form for $W(h;\xi,r)$. The derivation of an expression for W is nontrivial, and it is here where approximations enter the theory. Katchalsky and Lifson used for W a function developed by Katchalsky,[35] which is based on two major assumptions. First, the polymer end-to-end distance probability, along with the distance probability between any pair of fixed charges, is represented by a Gaussian distribution. Second, the mean-square end-to-end distance, $\langle r^2\rangle$ (which appears in the probability distribution), is equated to that for the *unperturbed* chain, $\langle r_0^2\rangle$; similarly, the mean-square distance between any two charged segments is given by the fraction ξ of the mean-square end-to-end distance for the chain. The resulting expression is[35]

$$W(h;\xi,r) = \left[\frac{2}{3}\pi\langle r_0^2\rangle\xi(1-\xi)\right]^{-1/2}\frac{h}{r\kappa}\left[\exp\left(-\frac{3}{2}\frac{(h-\xi r)^2}{\langle r_0^2\rangle\xi(1-\xi)}\right) - \exp\left(-\frac{3}{2}\frac{(h+\xi r)^2}{\langle r_0^2\rangle\xi(1-\xi)}\right)\right] \tag{10}$$

Substituting eq 10 into eq 9 and performing the two integrations indicated in eqs 8 and 9, Katchalsky and Lifson obtain an expression for F_{el}. The exact form for F_{el} is a complicated integral equation which must be evaluated numerically. For most conditions of interest, this exact solution can be replaced by the approximate equation:[7]

$$F_{el} = \frac{\nu^2\epsilon^2}{Dr}\ln\left(1+\frac{6r}{\kappa\langle r_0^2\rangle}\right) \tag{11}$$

The degree of chain expansion is now determined by minimizing the polyion free energy (which includes an entropy term along with F_{el}) with respect to the end-to-end separation distance, r. The resulting expression is usually written in terms of the expansion factor, α^2, which is the ratio of the mean-square end-to-end distance for the real (expanded) polyion to that for the unperturbed chain, i.e., $\alpha^2 = \langle r^2\rangle/\langle r_0^2\rangle$. The K–L expression for F_{el} gives for the expansion factor[9]

$$\alpha^2 - 1 = \frac{\nu^2\epsilon^2}{3DkT\langle r_0^2\rangle^{1/2}\alpha}\left[\ln\left(1+\frac{6\alpha}{\kappa\langle r_0^2\rangle^{1/2}}\right) - \frac{6\alpha/\kappa\langle r_0^2\rangle^{1/2}}{1+6\alpha/\kappa\langle r_0^2\rangle^{1/2}}\right] \tag{12}$$

Equation 12 is sometimes replaced by a limiting form valid for high molecular weights and/or high ionic strength.[9,11] Here we are interested in a range of system conditions and thus retain the full form of eq 12 for our comparison.

Equations 11 and 12 are based implicitly on the two assumptions used in deriving eq 10, neither of which is justified a priori. The assumption that $\langle r_0^2\rangle$ is the mean-square end-to-end distance of the chain is inconsistent with our knowledge (and predictions of eq 12) that electrostatic interactions perturb the polyion, causing it to expand. This inconsistency in the K–L theory was removed[9,11] by assuming that the polyion expands uniformly during the

Table VII
Average Percent Differences between Simulation Results and Theoretical Predictions for Electrostatic Energies and Expansion Factors

	electrostatic energy		expansion factor	
N	K–L[a]	uniform exp[b]	K–L[a]	uniform exp[b]
20	442	280	125	105
40	561	251	164	114
60	502	183	180	112
100	700	262	171	97.9
140	917	318	111	83.3

[a] Katchalsky–Lifson theory.[7] [b] Uniform-expansion extension of Katchalsky–Lifson theory.[9]

charging process and by replacing $\langle r_0^2 \rangle$ in eq 10 with $\langle r^2 \rangle = \alpha^2 \langle r_0^2 \rangle$. Consistency is thus imposed in the theory by using the correct (but, yet unknown) mean separation distance in eq 10. However, as in eq 10, the distance probabilities are described by using Gaussian distribution functions. The resulting expression for the electrostatic energy in this extended version of K–L theory is[9]

$$F_{el} = \frac{\nu^2 \epsilon^2}{Dr} \ln\left(1 + \frac{6r}{\alpha^2 \langle r_0^2 \rangle \kappa}\right) \tag{13}$$

and for the expansion factor[9]

$$\alpha^2 - 1 = \frac{\nu^2 \epsilon^2}{3DkT \langle r_0^2 \rangle^{1/2} \alpha}\left[\ln\left(1 + \frac{6}{\kappa\alpha \langle r_0^2 \rangle^{1/2}}\right) + \frac{6/\kappa\alpha \langle r_0^2 \rangle^{1/2}}{1 + 6/\kappa\alpha \langle r_0^2 \rangle^{1/2}}\right] \tag{14}$$

Equations 13 and 14 are referred to as the *uniform-expansion* extension of K–L theory.

We compare simulation results for the mean electrostatic energy, $\langle E \rangle$, and expansion factor α^2 with predictions based on eqs 11–14. For comparing $\langle E \rangle$ with predictions for F_{el}, we use for r in eqs 11 and 13 the *mean* end-to-end distance calculated from the simulation. We also use in eq 13 the simulation result for α^2. All other parameters in eqs 11–14 (e.g., κ, ν^2, and D) correspond to specified system conditions and are identical with values used in the simulation. Predictions for α^2 are obtained by solving the roots of eqs 12 and 14 for specified conditions.

Before presenting comparisons, we note that eqs 11–14 are valid for *finite* screening lengths and not in the limit of $\kappa = 0$. Katchalsky and Lifson[7] derived an expression for F_{el} that can be used to determine the corresponding versions for eqs 11–14 in the unscreened limit. To avoid complicating our discussion, we limit attention here to the four *finite* screening lengths examined in the simulation.

Table VII gives average percent differences between theoretical and simulated electrostatic energies and expansion factors for the five chain lengths studied. The tabulated percent differences are averages over the range of (finite) screening lengths and charge densities examined for each chain length. Two conclusions are immediately evident from Table VII. First, both theories give order-of-magnitude errors for $\langle F_{el} \rangle$ and α^2 when compared with simulation. Second, as expected, the uniform-expansion extension of K–L theory gives improved results over the original K–L theory; however, this improvement still results in less than semiquantitative predictions.

Figures 8 and 9 present graphical comparisons of simulation and theory for 100-segment chains at $\kappa^{-1} = 3.04$ and 96.2 Å. The results in these figures are representative of those obtained for other chain and screening lengths. Some observations not directly evident from Table VII now become clear. Both theories predict the correct trends in F_{el} and α^2 with varying chain ionization and screening length. K–L theory always overestimates F_{el} (Figure 8); uniform-expansion theory overpredicts F_{el} at low ionization but *underpredicts* F_{el} at high chain extensions (high ionization, large screening length). Predicted expansion factors (Figure 9) also exceed simulation results for most conditions.

From our comparison, we conclude that the K–L and uniform-expansion theories represent only qualitatively the configurational properties of the physical model on which they are based. The most questionable assumptions

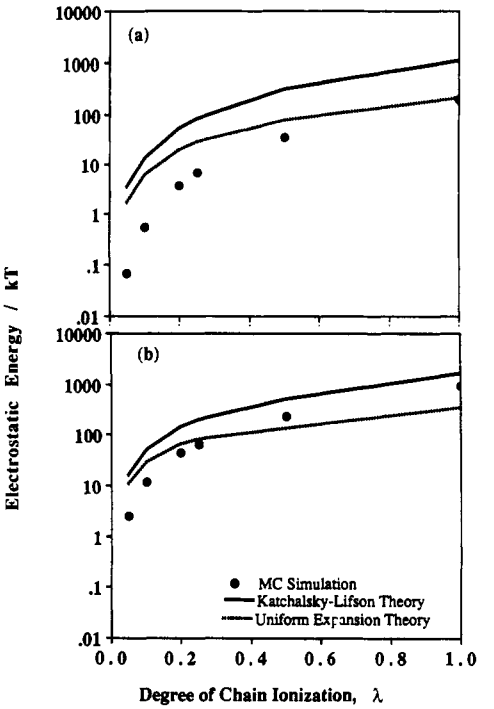

Figure 8. Comparison of simulated and predicted electrostatic energies for partially ionized 100-segment chains: (a) screening length $\kappa^{-1} = 3.04$ Å; (b) screening length $\kappa^{-1} = 96.2$ Å.

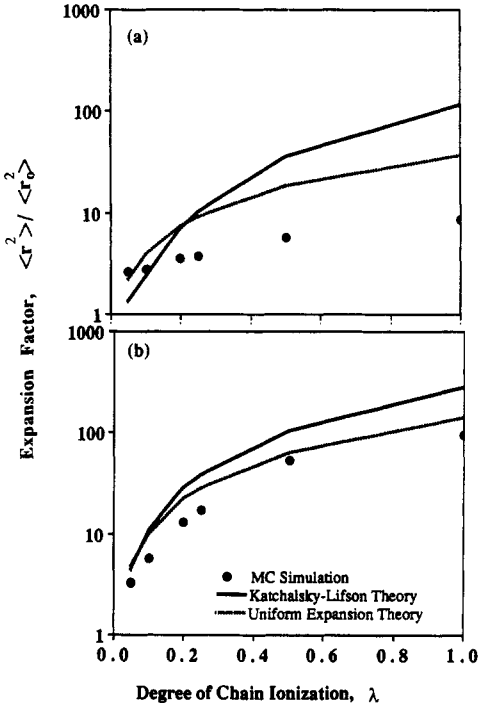

Figure 9. Comparison of simulated and predicted expansion factors for partially ionized 100-segment chains: (a) screening length $\kappa^{-1} = 3.04$ Å; (b) screening length $\kappa^{-1} = 96.2$ Å.

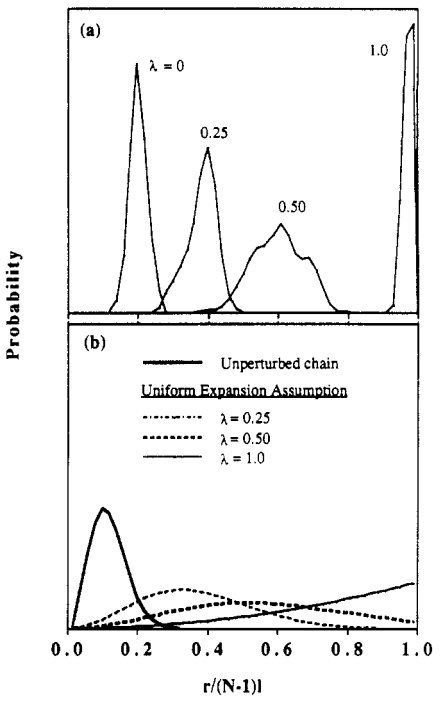

Figure 10. Probability distributions for end-to-end distance r for 60-segment chains at κ^{-1} = 30.4 Å: (a) simulation; (b) theory.

in the derivation of the two theories occur in the choice of $W(h;\xi,r)$, the probability distribution for finding a distance h between two segments (represented by ξ) when the polyion end-to-end distance is r. The theories make a priori assumptions regarding this distribution; in the simulation, the distribution is generated in the Monte Carlo search over configurational space. We have analyzed the simulation-generated distributions (section II.C) for the case ξ = 1, i.e., the distribution for the polyion end-to-end distance.

Figure 10a presents end-to-end distance distributions calculated from simulation for 60-segment chains at κ^{-1} = 30.4 and $0 \leq \lambda \leq 1$. Figure 10b gives the corresponding distributions predicted by the theories. The theoretical distributions were normalized in a manner analogous to that for the simulation results, and the vertical axes in Figure 10 have the same scale. The simulation results indicate a shifting of the distribution to more stretched conformations which occurs with increasing chain ionization. The distribution broadens slightly for intermediate ionizations and then forms a sharp spike around an extended (rodlike) conformation for the fully ionized chain.

The K–L assumption for the end-to-end distance distribution of a 60-segment chain is represented in Figure 10b by the curve for the unperturbed chain. The unperturbed chain is not affected by electrostatic interactions; thus, separation distances between charged groups (along with the end-to-end distance) for this chain are smaller than those for the case (Figure 10a) where charged groups interact. Because the K–L expression for W assumes an unrealistically close separation between ionized groups, predicted electrostatic energies are higher than those from simulation calculations (Figure 8).

Uniform-expansion theory uses in the expression for W the mean end-to-end distance for the *perturbed* chain. Thus, this theory contains a self-consistent dependence of the mean end-to-end distance on the electrostatic perturbations; however, the *distribution* about this mean is represented by a Gaussian function. On substituting the mean end-to-end distance for the perturbed chain into a Gaussian expression for the distance distribution, we obtain the distribution curves in Figure 10b. The distributions in Figure 10b for λ = 0.25, 0.50, and 1.0 have the same *mean* values as the corresponding distributions in Figure 10a but are much broader. The Gaussian distribution becomes particularly unrealistic at high chain extensions where end-to-end distances larger than the maximum possible extension are allowed.

It is clear from Figure 10 that neither theory provides a reasonable estimate of the end-to-end distance distribution for ionized chains and thus for the distance distributions between ionized segments on the chains. We believe it is this inadequate description of $W(h;\xi,r)$ that accounts for the poor agreement between theoretical and simulated electrostatic energies and expansion factors. The obvious solution for testing this conclusion, and for improving agreement between theory and simulation, is to use an expression for W that is consistent with the simulation-generated distance distributions. This proposal is conceptually trivial, but mathematically complex. It is the (relatively) simple form of eq 10 that makes the two integrations of eq 8 and 9 tractable. A realistic expression for W, which accounts for the coupled dependences of all relevant length scales on the distance distributions, would not only be difficult to obtain in analytical form but equally difficult to integrate through eqs 8 and 9.

An alternative to correcting the theory from first principles (i.e., by starting with "correct" distribution functions) would be to concentrate directly on the final expression for F_{el}. It is this expression (specifically the derivative $\partial F_{el}/\partial r$) that determines the predictions for polyion configurational properties. If the dependence of F_{el} on polyion end-to-end distance r is described accurately, e.g., by a semiempirical relation or by a correction to eq 11, then expansion-factor predictions should agree well with simulation. Our simulation results are not appropriate for determining the dependence of F_{el} on r because r assumes a distribution of values over the course of the simulation (Figure 10). For accurate determination of the dependence of F_{el} on r, it would be more appropriate to calculate ensemble averages of $\langle E \rangle$ at different (fixed) values of r; this calculation would require holding the chain ends fixed in the simulation and allowing internal chain motions in order to sample over configurational space.

V. Conclusions

Using Monte Carlo simulation we have studied the conformational properties of a simple lattice representation of isolated, partially ionized polyelectrolytes. The calculated dependence of polyion properties on system length scales is complex; the behavior of the chains ranges from flexible to rodlike, depending on chain length, charge density, and screening length. Power law scaling behavior was observed only at high charge screenings (κ^{-1} = 3.04 Å); at lower screenings, intermediate length dependence of configurational properties was observed.

We compare our simulation results for electrostatic energies and expansion factors with theoretical predictions based on a model directly analogous to that studied in the simulation. We observe large differences between theory and simulation and credit these discrepancies to inaccurate theoretical descriptions of the distance probability distributions between ionized segments.

The polyelectrolyte model studied in this work is simple and neglects the detailed features of a real polyion in the presence of discrete solvent and counterions. However, theoretical descriptions of polyelectrolyte properties are necessarily based on simplified models of this type, and

the simulation results presented here provide a basis for developing and testing analytical theories. In addition, the model used here can be readily extended for considering more complex polyelectrolyte systems. In a forthcoming paper[27] we apply an extension of this model for examining the effect of short-range (nonelectrostatic) interactions on polyelectrolyte configurational properties.

Acknowledgment. This work was supported by the Director, Office of Energy Research, Office of Basic Energy Sciences, Chemical Sciences Division of the U.S. Department of Energy under Contract No. DE-AC03-76SF00098. The calculations reported here were performed on the IBM 3090 at the University of California at Berkeley Computing Center; we acknowledge the generous computation time provided by the Computing Center which made this work possible. The authors are grateful to Alexander Sassi for helpful assistance with the computer programming, and to Kevin Mansfield and Doros Theodorou for many fruitful discussions.

References and Notes

(1) Yamakawa, H. *Modern Theory of Polymer Solutions*; Harper & Row: New York, 1971.
(2) de Gennes, P.-G. *Scaling Concepts in Polymer Physics*; Cornell University Press: Ithaca, NY, 1979.
(3) Freed, K. F. *Renormalization Group Theory of Macromolecules*; John Wiley and Sons: New York, 1987.
(4) Rice, S. A.; Nagasawa, M. *Polyelectrolyte Solutions*; Academic: New York, 1961.
(5) Oosawa, F. *Polyelectrolytes*; Marcel Dekker: New York, 1971.
(6) Harris, F. E.; Rice, S. A. *J. Chem. Phys.* **1954**, *58*, 725.
(7) Katchalsky, A.; Lifson, S. *J. Polym. Sci.* **1953**, *11*, 409.
(8) Manning, G. S. *J. Chem. Phys.* **1969**, *51*, 924.
(9) Noda, I.; Tsunge, T.; Nagasawa, M. *J. Phys. Chem.* **1970**, *74*, 711.
(10) de Gennes, P.-G.; Pincus, P.; Velasco, R. M.; Brochard, F. *J. Phys. (Paris)* **1976**, *37*, 1461.
(11) Bailey, J. M. *Macromolecules* **1977**, *10*, 725.
(12) Skolnick, J.; Fixman, M. *Macromolecules* **1977**, *10*, 944.
(13) Odijk, T.; Houwaart, A. C. *J. Polym. Sci., Polym. Phys. Ed.* **1978**, *16*, 627.
(14) Soumpasis, D. M.; Bennemann, K. H. *Macromolecules* **1981**, *14*, 50.
(15) Le Bret, M. *J. Chem. Phys.* **1982**, *76*, 6243.
(16) Kholodenko, A. L.; Freed, K. F. *J. Chem. Phys.* **1983**, *78*, 7412.
(17) Bawendi, M. G.; Freed, K. F. *J. Chem. Phys.* **1986**, *84*, 449.
(18) Chen, Y.; Kholodenko, A. L. *J. Chem. Phys.* **1987**, *86*, 1540.
(19) Muthukumar, M. *J. Chem. Phys.* **1987**, *86*, 7230.
(20) See, for example: Kremer, K.; Baumgartner, A.; Binder, K. *J. Phys. A* **1981**, *15*, 2879. Kolinski, A.; Skolnick, J.; Yaris, R. *J. Chem. Phys.* **1986**, *85*, 3585. Karawawa, N.; Goddard, W. A. *J. Phys. Chem.* **1988**, *92*, 5828. Meirovitch, H.; Lim, H. A. *J. Chem. Phys.* **1989**, *91*, 2544.
(21) Brender, C.; Lax, M.; Windwer, S. *J. Chem. Phys.* **1981**, *74*, 2526.
(22) Brender, C.; Lax, M.; Windwer, S. *J. Chem. Phys.* **1984**, *80*, 886.
(23) Baumgartner, A. *J. Phys. Lett.* **1984**, *45*, L-515.
(24) Carnie, S. L.; Christos, G. A.; Creamor, T. P. *J. Chem. Phys.* **1988**, *89*, 6484.
(25) Christos, G. A.; Carnie, S. L. *J. Chem. Phys.* **1989**, *91*, 439.
(26) Valleau, J. P. *Chem. Phys.* **1989**, *129*, 163.
(27) Hooper, H. H.; Beltran, S.; Sassi, A.; Blanch, H. W.; Prausnitz, J. M. *J. Chem. Phys.* **1990**, *93*, 2715.
(28) Rieger, P. H. *Electrochemistry*; Prentice-Hall: Englewood Cliffs, NJ, 1987.
(29) Metropolis, N.; Rosenbluth, A. W.; Rosenbluth, M. N.; Teller, A. H.; Teller, E. J. *J. Chem. Phys.* **1953**, *21*, 1087.
(30) Wall, F. T.; Mandel, F. *J. Chem. Phys.* **1975**, *63*, 4592.
(31) Smith, E. B.; Wells, B. H. *Mol. Phys.* **1984**, *53*, 701.
(32) Katchalsky, A.; Michaeli, I. *J. Polym. Sci.* **1955**, *15*, 69. Ilavsky, M. *Polymer* **1981**, *22*, 1687. Ilavsky, M.; Hrouz, J.; Havlicek, I. *Polymer* **1985**, *26*, 1514.
(33) Hooper, H. H.; Baker, J. P.; Blanch, H. W.; Prausnitz, J. M. *Macromolecules* **1990**, *23*, 1096.
(34) Beltran, S.; Hooper, H. H.; Blanch, H. W.; Prausnitz, J. M. *J. Chem. Phys.* **1990**, *92*, 2061.
(35) Katchalsky, A. *J. Polym. Sci.* **1951**, *7*, 393.